

# CO<sub>2</sub> absorption through PP/fSiO<sub>2</sub> nanocomposite hollow fiber membrane contactor

Saba Raveshiyan<sup>1,2</sup>, Parya Amirabedi<sup>3</sup>, Reza Yegani<sup>1,2\*</sup>, Behzad Pourabbas<sup>4</sup>,  
Akram Tavakoli<sup>1</sup>

<sup>1</sup>Faculty of Chemical Engineering, Sahand University of Technology, Tabriz, Iran

<sup>2</sup>Membrane Technology Research Center, Sahand University of Technology, Tabriz, Iran

<sup>3</sup>Faculty of Engineering, Behbahan Khatam Alanbia University of Technology, Behbahan, Iran

<sup>4</sup>Department of Polymer Engineering., Sahand University of Technology, Tabriz-Iran

Received: 30 October 2021, Accepted: 18 December 2021

## ABSTRACT

Wetting of polymeric hollow fiber membranes by chemical absorbents is one of the main challenges of gas-liquid membrane contactors. This study explored an appropriate method to fabricate a superhydrophobic polypropylene (PP) hollow fiber membrane by incorporating fluorinated silica nanoparticles (fSiO<sub>2</sub> NPs) on the PP membrane surface. The effect of the hydrophobic agent on the water repellent properties of the composite membrane was studied by varying (1H,1H,2H,2H-perfluorooctyltriethoxysilane/ tetraethylorthosilicate) (PFOTES/TEOS) molar ratio from 0 to 1. The composite membranes were characterized using field emission scanning electron microscopy (FESEM), attenuated total reflection-Fourier transform infrared (ATR-FTIR), contact angle, mechanical strength and static wettability. The obtained results showed that the surface hydrophobicity and mechanical strength of the composite membranes increased compared to pure ones. The contact angle of 156° was obtained when the (PFOTES/TEOS) molar ratio was 0.5. Furthermore, the CO<sub>2</sub> absorption experiment was done to evaluate the performance of the fabricated membranes in a gas-liquid membrane contactor. The obtained results showed that the PP/fSiO<sub>2</sub> composite membrane has more potential to be used in gas-liquid membrane contactors than commonly used polymeric membranes. **Polyolefins J (2022) 9: 61-71**

**Keywords:** Superhydrophobic; polypropylene membrane; fluorinated silica nanoparticles; membrane contactor; wettability.

## INTRODUCTION

Lotus leaf is one of the natural superhydrophobic surfaces. In lotus leaves, the combination of rough micro and nanoscale binary structure and hydrophobic wax surface leads to self-cleaning properties. [1,2]. Recent research has indicated that hydrophobic materials have attracted great interest in most fields such as membrane-based technology [3-5].

Gas-liquid membrane contactor is one of the main

membrane applications utilizing hydrophobic hollow fiber membranes. In this system, hollow fiber membrane acts as an interface barrier between the liquid phase and gas phase and provides a large contacting area between these two phases. Some of the chief benefits of hollow fiber membrane contactors are great surface-area to volume ratio, linear scale-up, modularity and operating flexibility. However, the wetting of membranes due to

\*Corresponding Author - E-mail: ryegani@sut.ac.ir

the penetration of liquid adsorbent is the most important challenge of membrane contactors, which causes a severe drop in their performance.[5-8]. Thus, in order to increase the efficiency of this equipment, it is necessary to increase the hydrophobicity and chemical stability of the membranes [9].

There are many methods to increase the hydrophobicity and chemical stability of polymeric membranes, which sol-gel is the most important method. It should be noted that many parameters in the sol-gel process affect the synthesis of nanoparticles, so precise control of these parameters can fabricate a surface with high hydrophobicity [10-12].

Wang et al. prepared hydrophobic polyetherimide hollow fiber membrane through the coating of the fluorinated silica NPs on the surface of the membranes via the sol-gel process. The experimental results revealed that the coating of the fluorinated silica nanoparticles greatly improved the hydrophobicity and chemical stability of these membranes [9]. Wang et al. fabricated PP composite membranes by loading SiO<sub>2</sub> NPs and attaching 1H,1H,2H,2H-perfluoro decyltriethoxysilane (PFOTS) on the membrane sample surface to be used in vacuum membrane distillation (VMD) [13]. In our previous works, a superhydrophobic composite hollow fiber membrane was produced by incorporation of the CH<sub>3</sub>-g-silica NPs on the PP hollow fiber membrane and the fabricated membrane was applied for CO<sub>2</sub> absorption using membrane contactor [14,15]. Results showed that the incorporation of the CH<sub>3</sub>-g-silica NPs on the surface of PP membrane not only caused superhydrophobicity but also would keep the polymeric membrane away from the attacks of liquid absorbents.

Over the past two decades, polypropylene has been used as one of the most commercial symmetrical hollow fiber membrane contactor materials. Polypropylene has excellent characteristics such as balanced physical and mechanical properties, high resistance to water and chemical environments, excellent processability, low cost and so on. Hence, expansion of the application area of PP membranes is highly desired [16,17].

Due to the importance of hydrophobicity of polypropylene membranes in membrane contactors, we used fluorinated silica NPs to fabricate superhydrophobic polypropylene hollow fiber membrane for CO<sub>2</sub> absorption.

The fluorination method is one of the important hydrophobic surface modifications of polymeric surfaces. Fluorinated polymer surfaces have been widely considered for their low surface energies and subsequently, their lower wetting tendencies. Most reported fluorination techniques in the literature include melt blending of polymers with fluoro chemicals and plasma surface treatments [18]. Hence, in this work, we used a different and appropriate method to fluoridate the surface of polypropylene membrane.

Fluorinated silica NPs were synthesized via hydrolysis and condensation of TEOS and PFOTES using one-step sol-gel process. The effects of inorganic NPs loading on the membranes' morphology, mechanical stability and CO<sub>2</sub> absorption flux were investigated. The main novelty of the current work is the investigation of PFOTES/TEOS molar ratio on the structural properties and CO<sub>2</sub> absorption performance of the PP composite hollow fiber membranes, which no study has been reported yet. The synthesized fabricated membranes were characterized by various characterization analyses, including ATR-FTIR, FESEM, porosity, contact angle and mechanical strength.

## EXPERIMENTAL

### Materials

Tetraethylorthosilicate (TEOS), perfluorooctyltriethoxysilane (PFOTES), methanol (MeOH) and ammonium hydroxide (NH<sub>4</sub>OH), used for NPs synthesis, were purchased from Merck. Hydrogen peroxide (H<sub>2</sub>O<sub>2</sub>) and sulfuric acid (H<sub>2</sub>SO<sub>4</sub>), used to prepare the Piranha solution and monoethanolamine (MEA) as well as diethanolamine (DEA) as a chemical absorbent were purchased from Merck. Isotactic polypropylene (iPP, EPD60R, MFI = 0.35 g/10 min) as a membrane matrix material was provided from Arak Petrochemical Company of Iran. Irganox 1010 as a heat stabilizer, mineral oil (MO) as a diluent and acetone as an extractor were purchased from CibaCo., Acros Organics and Merck, respectively.

### Hollow fiber membrane preparation

First PP granules were dried for at least 5 h at 75°C before hollow fiber membrane fabrication. The hollow

fiber membranes were fabricated by thermally induced phase separation (TIPS) method. PP granules were added to the MO and melt-blended at 170°C for 100 min in a sealed glass vessel to achieve a homogeneous solution. After degassing; the prepared solution, the dope solution and bore fluids were extruded through a spinneret and went through an air gap before immersing into a water bath. The spinning conditions were summarized in Table 1. The nascent fibers were collected using a rotating drum and subsequently immersed in acetone for 24 h to extract the MO and achieve a desired porous hollow fiber membrane.

### Preparation of composite hollow fiber membranes

According to the method explained in our previous work, in order to expose OH functional group, as a linkage agent between the synthesized particles and membrane surface, the porous hollow fiber membranes were treated by Piranha solution; (3:1 weight ratio of H<sub>2</sub>SO<sub>4</sub>:H<sub>2</sub>O<sub>2</sub> solution) for 3 hr [14]. All pretreated membranes were washed with deionized water (DI) and then dried at ambient temperature.

After pretreatment of membranes with Piranha solution, certain amounts of MeOH, TEOS, NH<sub>4</sub>OH and H<sub>2</sub>O were mixed for 1 h, at ambient temperature to obtain silica colloid particles. Then the desired amounts of PFOTES (varying (PFOTES/TEOS) molar ratio from 0 to 1) were added dropwise into the solution. The mixtures were stirred for 12 h at room temperature. Afterward, Piranha-treated hollow fiber

**Table 1.** Spinning conditions for fabrication of PP hollow fiber membranes.

Spinning conditions	Remarks
Air gap distance (cm)	1
Take up speed (rpm)	20
Bore flow rate (ml/min)	2.0
Bore fluid composition	MO
Bore fluid temperature	25 °C
Coagulation medium	water

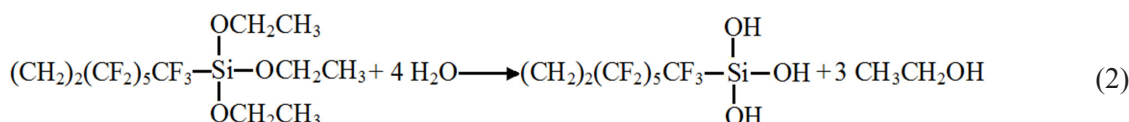
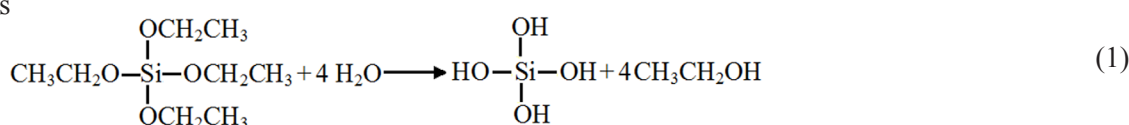
membranes were immersed in the mixture for 3 h and then dried at 75°C for 4 h. Finally, all the fabricated membranes were washed with deionized water under ultrasonication and dried before analysis.

### Reaction mechanism of the sol-gel process

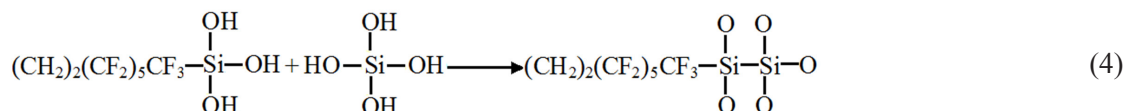
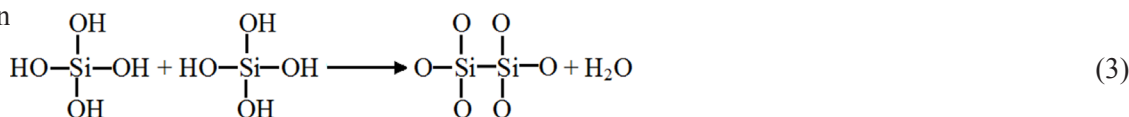
fSiO<sub>2</sub> NPs were synthesized by hydrolysis and condensation of alkoxy silanes in a mixture of MeOH, H<sub>2</sub>O and NH<sub>4</sub>OH. The chemical reaction showing the hydrolysis and condensation of TEOS and PFOTES is briefly written as equations 1-4 [19]:

According to equations (1) and (3), TEOS can be hydrolyzed and condensed to generate silica nanoparticles (SiO<sub>2</sub> NPs). By adding PFOTES inside the solution containing silica colloid particles, the ethoxy groups of PFOTES are instantly hydrolyzed. Subsequently, the condensation reaction can occur between the hydrolyzed PFOTES molecules and the active hydroxyl groups present on the surface of silica nanoparticles [20]. After surface modification of the silica nanoparticles with the hydrophobic fluorine agent and the formation of fluorinated silica nanopar-

Hydrolysis



Condensation



ticles, Piranha-treated hollow fiber membranes were dipped inside the sol solution. In this stage, fluorinated silica nanoparticles could form hydrogen bonds with the hydroxyl groups of the Piranha-treated membranes.

## Membrane Characterizations

### ATR-FTIR analysis

Chemical structures of the pure and composite hollow fiber membranes were analyzed by the attenuated total reflection-Fourier transform infrared (ATR-FTIR) spectra using an infrared spectroscopy device (Bruker, TENSOR27, Germany) in the range of 500-4000 cm<sup>-1</sup>.

### FESEM analysis

The outer surface and cross-section structure of fibers were observed by the field emission scanning electron microscopy (FESEM) from Tescan (USA). Before observation, the samples were broken in liquid nitrogen and then coated with gold by sputtering to make conductive them.

### Porosity analysis

The fibers were first cut to specific lengths and then immersed in isobutanol for 24 hours to fill their pores with liquid. In general, the porosity ( $\varepsilon$ ) of membrane samples is defined as the volume of the pore divided by the total volume of the membrane using the following equation [21]:

$$\varepsilon = \frac{(w_w - w_d) / \rho_w}{(w_w - w_d) / \rho_w + (w_d / \rho_d)} \times 100 \quad (5)$$

where  $w_w$  is the mass of the isobutanol-impregnated membrane (g),  $w_d$  is the mass of the dry membrane (g),  $\rho_w$  is the isobutanol density and  $\rho_d$  is the density of the polypropylene. In this work, the densities of polypropylene and isobutanol were considered 0.9 and 0.86 (g/cm<sup>3</sup>), respectively.

### Contact angle

The static contact angle of the pure and nanocomposite membrane samples was measured using a contact angle goniometer (PGX, Thwing-Albert Instrument Co, USA). For each membrane sample, the static contact angle was measured at five different spots and the values were averaged.

### Mechanical strength analysis

The mechanical properties of the pure and nanocomposite membrane samples were evaluated using a tensile machine (STM-5, SANTAM, IRAN). The stretch speed was kept constant at 10 mm/min and the initial length of each fiber was adjusted at 15 cm. For each sample, three measurements were taken and the average value was reported.

### Static wettability

Static wettability studies were done according to the measurement of the weights of immersing pure and coated membranes in liquid absorbent solutions. Membranes were immersed in deionized water (DI) and an aqueous solution of MEA as well as DEA (both 30 wt%). At the end of the immersion time, all of the pure and nanocomposite membrane samples were taken out and were weighed. Then, the difference between the wet and dry weight of the membrane was reported as a volume of absorbed liquid solution.

### Membrane contactor experiments

To evaluate the performance of the prepared neat and composite hollow fiber membranes, CO<sub>2</sub> absorption experiment was done inside the membrane contactor. In this case, ten fibers were sealed in a cylindrical Plexiglas module. MEA (30 wt%) was used as a liquid absorbent. For all experiments, the absorbent flowed through the shell side whereas pure CO<sub>2</sub>, as well as mixed CO<sub>2</sub> gas (CO<sub>2</sub>/CH<sub>4</sub> 20/80 vol. %) flowed counter-currently through the lumen side of the hollow fiber membranes. The gas flow rates at the outlet and the inlet of the module were measured by soap film flow meters (HORIBA STEC- VP-3). The gas-side pressure was adjusted at 1 bar where the liquid pressure was set 0.5 bar higher to avoid the bubble formation in the liquid phase [22]. Finally, for pure CO<sub>2</sub>, the absorbent flows concentrations of the inlet and outlet streams were measured by titration method [23].

In order to analyze the mixed gas compositions, gas chromatography (GC) was employed. The CO<sub>2</sub> removal efficiency and absorption flux were calculated by equations (6) and (7), respectively [24]:

$$\varepsilon = \frac{Q_{g\ in} \times C_{g\ in} - Q_{g\ out} \times C_{g\ out}}{Q_{g\ in} \times C_{g\ in}} \quad (6)$$

$$J = \frac{(Q_{g\ in} \times C_{g\ in} - Q_{g\ out} \times C_{g\ out}) \times 273.15}{0.0224 \times T_g \times S} \quad (7)$$

where  $\varepsilon$  is the  $\text{CO}_2$  removal efficiency (%);  $J$  is the flux of  $\text{CO}_2$  ( $\text{mol}/\text{m}^2\text{s}$ );  $Q_{gin}$  and  $Q_{gout}$  are the gas flow rates at the inlet and the outlet, respectively ( $\text{m}^3/\text{s}$ );  $Q_{gin}$  and  $Q_{gout}$  are the  $\text{CO}_2$  volumetric concentrations in the gas phase at the inlet and the outlet, respectively (%).  $T_g$  is the temperature of the feed gas (K) and  $S$  is the gas-liquid interfacial area ( $\text{m}^2$ ). The detailed information on the membrane contactor module was shown in Table 2.

## RESULTS AND DISCUSSION

### ATR-FTIR studies of the membrane

To investigate the chemical structure of the composite membranes with the various compositions of PFOTES/TEOS ratios, ATR-FTIR spectra of composite membranes were obtained and compared with those of pure PP membrane. As shown in Figure 1, the absorption bands at  $2950\text{--}2700\text{ cm}^{-1}$  are due to C-H stretching vibrations and the bands appeared at  $1376\text{ cm}^{-1}$  and  $1460\text{ cm}^{-1}$  confirm the bending the vibrations of C-H bond [25,26]. Comparing Figure 1a with Figure 1b indicates that in Figure 1b, the absorption bands have been almost omitted in 0% PFOTES due to the bending vibration of C-H bonds. In Figure 1b, the O-H stretching band at  $3358\text{ cm}^{-1}$  has appeared in the pretreatment step. After coating the samples, the absorption bands at  $800\text{--}700\text{ cm}^{-1}$  and  $1150\text{--}1020\text{ cm}^{-1}$  due to the Si-O asymmetric stretching vibrations and the bands at  $1000\text{--}900\text{ cm}^{-1}$  due to Si-OH were detected. The bands at  $1000\text{--}900\text{ cm}^{-1}$  and  $3358\text{ cm}^{-1}$  confirm the presence of unreacted TEOS, in which the O-H bonds provided by Piranha solution did not completely react with the Si-OH groups.

Comparing Figure 1a with Figs. 1c-f indicates that in the surface modification step, absorption bands due to

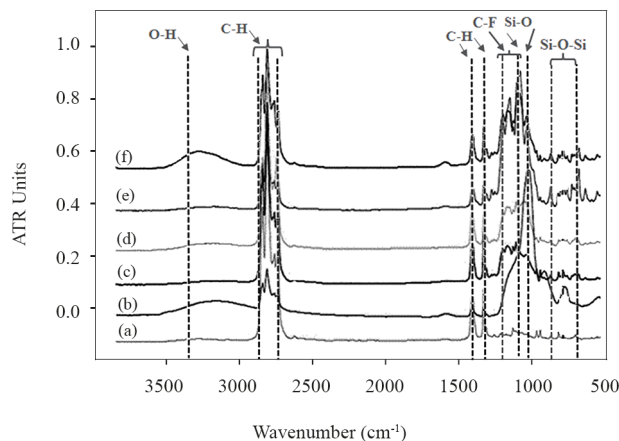


**Figure 1.** ATR-FTIR spectra of the PP membrane samples; (a) pure membrane, (b) composite membrane with (PFOTES/TEOS) = 0, (c) composite membrane with (PFOTES/TEOS) = 0.25, (d) composite membrane with (PFOTES/TEOS) = 0.5, (e) composite membrane with (PFOTES/TEOS) = 0.75, (f) composite membrane with (PFOTES/TEOS) = 1.

the C-H bonds have declined. The absorption bands in the range of  $1300\text{--}1100\text{ cm}^{-1}$  represent the C-F stretching vibrations and the absorption bands in the range of  $1145\text{ cm}^{-1}$  and  $800\text{--}700\text{ cm}^{-1}$  are related to the Si-O-Si bonds [27]. The band due to C-F bonds increases by enhancing PFOTES ratio in the mixture. When the molar ratio of PFOTES/TEOS is 1, the absorption band at  $3400\text{ cm}^{-1}$  shows that the surface OH groups have not completely reacted. Therefore, there is an optimal relative molar ratio of PFOTES to TEOS for lowering surface energy and increasing the roughness of the membrane.

### Membrane morphology observation

In Figure 2, the scanning electron microscopic images of the pure and composite membrane have been shown. According to Figure 2, the synthesis of fluorinated silica nanoparticles is observed on the membrane surfaces and also in the cross-sectional area of the membrane. Given the explained synthesis method, the solution has been coated on the outer surface of the membrane. Due to the porous structure of the membrane; the solution penetrates the porous structure of the membrane and nanoparticles have also been synthesized in pores. This indicates an open porosity that extends along with the cross-sectional area of the membrane. This point is the main advantage of using a porous membrane matrix in fabricating superhydrophobic membranes, which in addition to

**Table 2.** Specification of the hollow fiber modules.

Parameter	Value
Fiber outer dia. (mm)	0.7
Fiber inner dia. (mm)	0.5
Effective fiber length (cm)	18
Number of fibers	10
Module inner dia. (cm)	1
Module length (cm)	24

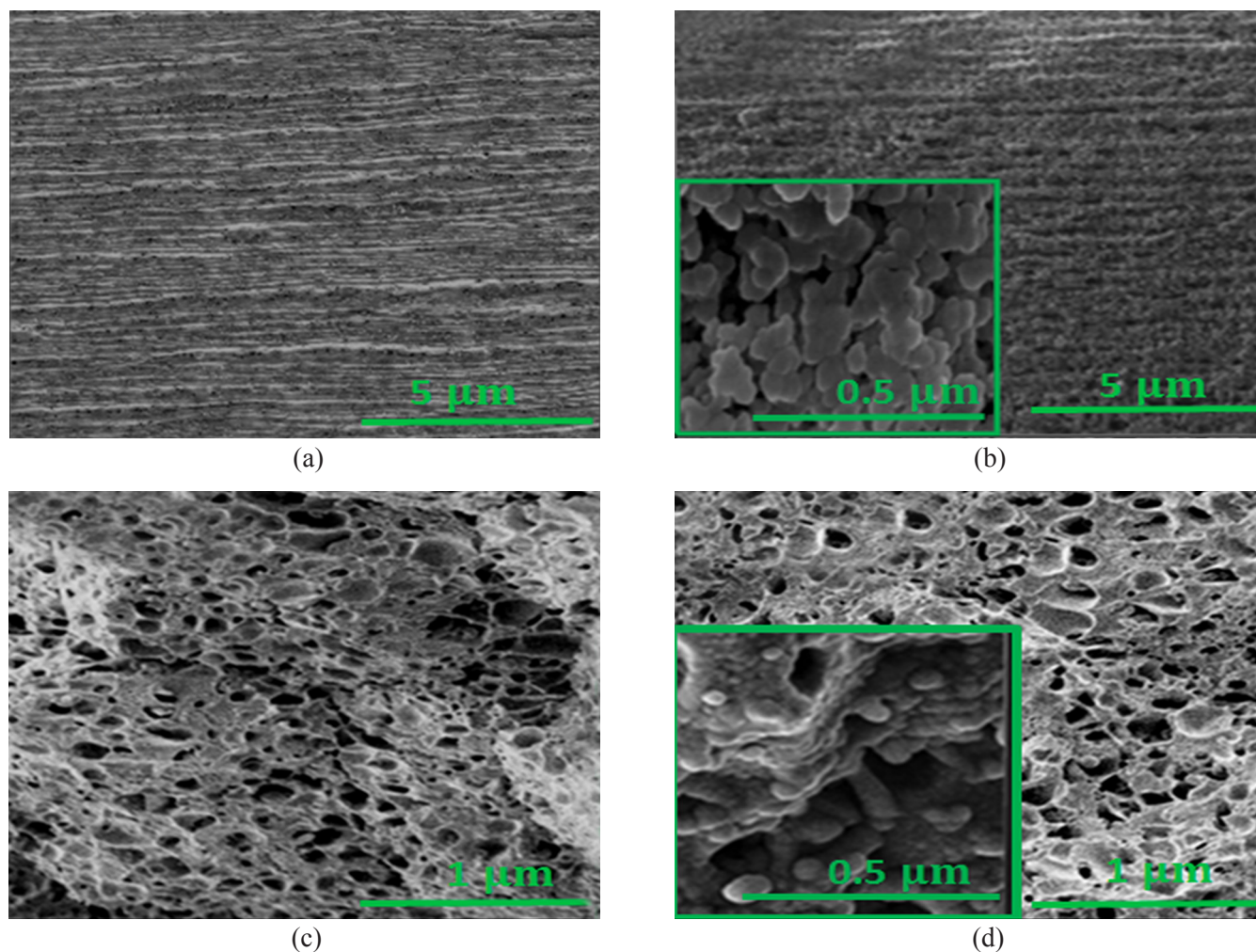


**Figure 2.** FESEM images of the PP membrane samples; (a) pure membrane and (b) composite membrane with (PFOTES/TEOS) = 0.5; (1) Cross section and (2) Outer surface.

the outer surface, the depth of membrane shows a superhydrophobic property. In other words, the synthesis of nanoparticles shows an appropriate distribution of hydrophobic properties in the surface and depth of the membrane.

#### Hydrophobicity of the composite membranes

Figure 3 shows changes in the surface contact angle of the samples prepared by different molar ratios of PFOTES/TEOS. The results indicate that when the molar ratio of PFOTES/TEOS increases to 0.5, the average contact angle increases to 156°. A surface with a contact angle higher than 150° is generally considered as a superhydrophobic surface. Therefore, when the PFOTES/TEOS molar ratio reaches 0.5, a superhydrophobic PP membrane is obtained. In coating by pure TEOS (without PFOTES), a sharp reduction

in contact angle from 125 to 70° was observed due to the presence of hydrophilic Si-OH groups. According to the sol-gel reactions for coating the membranes, the formation of nanoparticles takes place gradually. During the process, the primarily formed silica nanoparticles react with Si-OH groups to form new Si-O-Si bonds leading to more nanoparticles and surface roughness. Although the increase in roughness in inherently hydrophobic materials such as PP leads to an increase in hydrophobicity; however, due to the hydrophilic property of the silica nanoparticles, the final result is the increased hydrophilicity.

In coatings made by 0.25 and 0.5 molar ratios of PFOTES/TEOS, the contact angle increased from 125 (uncoated PP membrane) to 144 and 156°, respectively. This indicates an increase in the hydrophobic property of the membrane. However, with further increase of

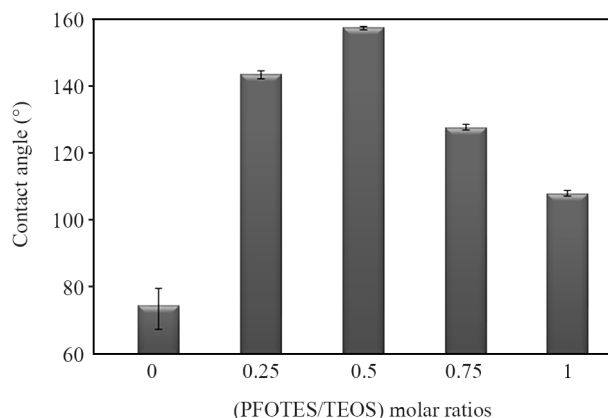


**Figure 3.** Water contact angles of the membrane samples prepared by different molar ratios of (PFOTES/TEOS).

PFOTES/TEOS molar ratios such as 0.75 and 1, the contact angle decreases to 128 and 107°, respectively. Therefore, it is concluded that when TEOS is reduced in the sol-gel mixtures, no primary silica nanoparticles are formed to be later modified by PFOTES for superhydrophobic purposes. In other words, TEOS is necessary for nanoparticle formation and therefore for the essential surface roughness for maximum hydrophobicity.

#### Mechanical properties of the composite membranes

Mechanical stability of the membranes is one of the important parameters for membrane contactor applications. Figure 4 shows the results of the mechanical strength test. All membranes coated with a solution containing PFOTES/TEOS show increased mechanical strength compared to pure polypropylene membrane. However, by increasing the molar ratio of PFOTES/TEOS, mechanical strength has regularly declined too. The samples coated with 0% of PFOTES have had the greatest increase in mechanical strength. This indicates that the reduction of TEOS content in the nanoparticles synthesis reduced the mechanical resistance of the nanoparticles. In other words, the amount of TEOS is an important parameter in determining the mechanical strength of nanoparticles [14].

The membrane coated with 0.5 PFOTES/TEOS molar ratio had the highest hydrophobicity and suitable mechanical strength in comparison with pure PP membranes. In order to perform other membrane analysis such as wettability, the membrane with 0.5 PFOTES/TEOS molar ratio was selected for the rest

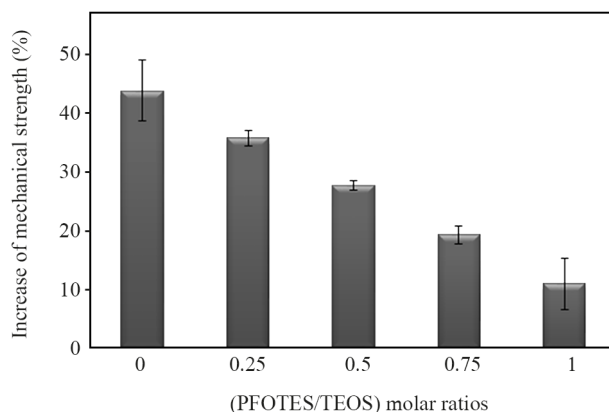


**Figure 4.** Increase of mechanical strength of the membrane samples prepared by different molar ratios of (PFOTES/TEOS).

of experiments.

#### Characterization of membrane static wettability

As mentioned before, improvement in hydrophobicity of the membrane has a great impact on the performance of membranes utilized in membrane contactors.

The measurement results of the static wettability for the membrane immersed in the three absorbents are plotted as a function of immersion time, as shown in Figure 5. Obviously, the weight of the immersed membrane continuously increased with the increase in immersion time. Compared to the raw samples, the amount of water absorption of the coated membrane in MEA, DEA and pure water reduced to 4, 2.5 and 2 times, respectively. Given that the coated samples contained fluorine atoms have lower surface energy, thus they prevent liquid absorbent entering into the pores of the membrane. According to Figure 5, the weight gain in DEA is higher than the other two adsorbents.

Since DEA has less surface tension compared with water and MEA, so the solution penetration into the pores of the membrane would be higher. It can be concluded that in wetting, surface tension plays an important role and the absorbents with lower surface tension show higher penetration into the membrane pores [28]. Weight gain in both coated and uncoated samples submerged in water is less than that of other adsorbents. The reason may lay behind the high surface tension of water than two other absorbents. Therefore, it penetrates less into the membrane pores.

Moreover, the static contact angle of the membrane samples immersed in the three absorbents plotted as

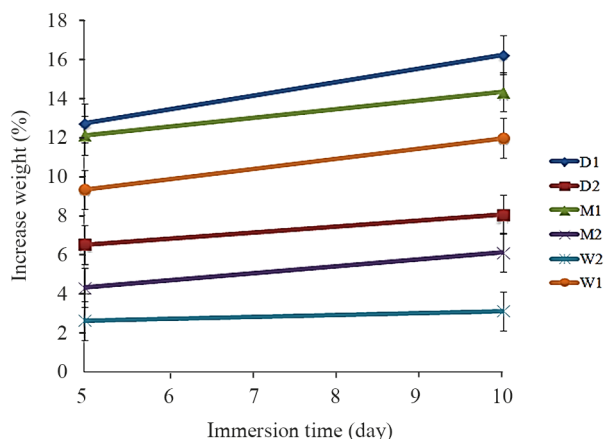


**Figure 5.** Increase of weight of the PP membrane samples immersing in DI (W) and aqueous solution of MEA (M) as well as DEA (D) for 10 days; (1) pure membrane and (2) composite membrane with (PFOTES/TEOS) =0.5.

a function of immersion time has been shown in Fig 6. Obviously, the static contact angle of immersing samples continuously reduced with the increase in immersion time. Coated samples reduced 7% and 10% of the contact angle after 5 and 10 immersion days, respectively. While typically a reduction of 10 % and 20% for uncoating samples were obtained. Drop in the static contact angle showed that fiber surface hydrophobicity significantly reduced due to immersion in liquid absorbent [29-31]. In this case, the absorbent molecules diffuse into the polypropylene membrane during immersion in the amine solution. Since the absorbent is hydrophilic, hydrophobicity and surface free energy decline when the absorbent molecules penetrate the fiber. Given that the reduction in static

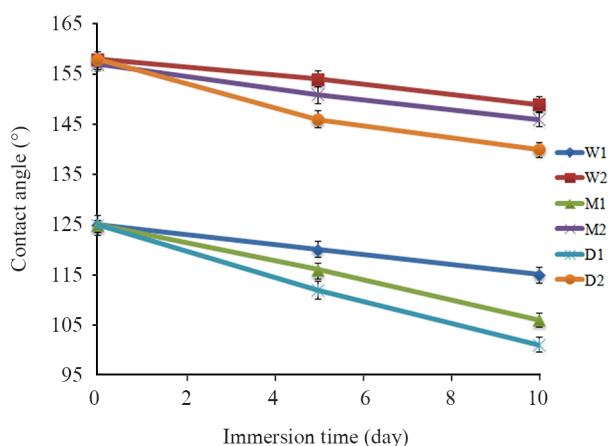


**Figure 6.** Static contact angle of the PP membrane samples immersing in DI (W) and aqueous solution of MEA (M) as well as DEA (D) for 10 days; (1) pure membrane and (2) composite membrane with (PFOTES/TEOS) =0.5.

contact angle is strongly reliant on the surface tension of the liquid absorbent, thus the absorbent with a poorer surface tension penetrates more easily into the fiber pores and results in partial wetting. Accordingly, the static contact angle for immersing samples in DI has been always the highest, whereas the static contact angle for samples immersed in MEA was higher than those immersed in DEA. It is necessary to mention, the contact angles of all coated membranes were still over 140° which means that each membrane still has a high hydrophobic surface.

### CO<sub>2</sub> absorption in membrane contactor

The CO<sub>2</sub> absorption performance of the neat and composite membranes is influenced by liquid flow rate. In order to investigate this issue, a mixture of CO<sub>2</sub> and CH<sub>4</sub> with composition of 20 % and 80 % mol, respectively, was considered as feed gas.

Since flow rate has a noticeable effect on the mass transfer rate of CO<sub>2</sub>, it is one of the most important parameters in the gas-liquid membrane contactors [24]. Figure 7 shows the results of CO<sub>2</sub> flux obtained at different liquid flow rates. CO<sub>2</sub> flux for both neat and composite membranes increased by increasing liquid flow rate. This is because that the boundary layer thickness of the liquid phase in the sell side is reduced by increasing the flow rate of liquid and the mass transfer coefficient, which results in reduced liquid phase resistance.

Further, Figure 7 displays that CO<sub>2</sub> flux in composite membranes is higher than that in pure ones, which can

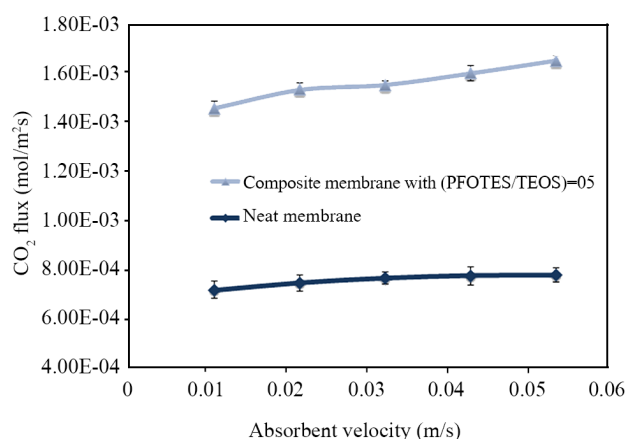


**Figure 7.** Effect of liquid flow rate on the CO<sub>2</sub> flux using MEA (30 wt. %) as the liquid absorbent (gas flow rate: 50 ml/min; CO<sub>2</sub> volume fraction in feed gas: 20 vol. %).

**Table 3.** Comparison of various membranes used for CO<sub>2</sub> absorption in membrane contactors.

Membrane	OD/ID (mm)	Pore size (μm)	Porosity (%)	CO <sub>2</sub> flux (mol m <sup>-2</sup> s <sup>-1</sup> )	Manufacturer	Ref.
PP	0.8/0.5	0.140	45	8.0×10 <sup>-4</sup>	In-house made	Current work
PP- fSiO <sub>2</sub>	0.8/0.5	0.127	44	1.57×10 <sup>-3</sup>	In-house made	Current work
PP-CH <sub>3</sub> SiO <sub>2</sub>	0.8/0.5	0.120	42	1.49×10 <sup>-3</sup>	In-house made	[14]
PP	0.3/0.22	0.040	40	1.4×10 <sup>-3</sup>	Celgard Inc.	[33]
PEI + fSiO <sub>2</sub>	0.8/1.1	0.040	81	8.68×10 <sup>-4</sup>	In-house made	[9]
PVDF + SMM	–	0.385	85	8×10 <sup>-4</sup>	In-house made	[36]
PSf + glycerol	0.5/1	0.01	72	7.5 × 10 <sup>-4</sup>	In-house made	[37]
PVDF + CaCO <sub>3</sub>	0.85-0.97/0.63-0.69	0.027	81	1.52×10 <sup>-3</sup>	In-house made	[35]

be attributed to the superhydrophobic surface of the composite membrane. In fact, the superhydrophobic surface of the composite membrane prevents membrane wetting under operational conditions [15].

### Comparison of CO<sub>2</sub> flux of different membranes used in membrane contactors

Table 3 shows the summary of the CO<sub>2</sub> flux of different membranes used in membrane contactors. At a liquid flow rate of 250 ml/min, the optimized PP/fSiO<sub>2</sub> composite membrane showed the highest CO<sub>2</sub> absorption flux of 1.49×10<sup>-3</sup> (mol/m<sup>2</sup>s). We can see that other polymeric membranes such as PP and PVDF [32], PP [33] PSf [34] show poorer CO<sub>2</sub> absorption performance than optimized PP/fSiO<sub>2</sub> composite membrane. In addition, it can be observed that the CaCO<sub>3</sub>/PVDF composite membrane [35] showed better CO<sub>2</sub> absorption flux than the conventional PP/fSiO<sub>2</sub> composite membrane due to the high porosity. However, the high porosity of CaCO<sub>3</sub>/PVDF composite membrane may reduce the wetting resistance of membrane compared with that of PP/fSiO<sub>2</sub> composite membrane.

Thus, the obtained results were promising, which means that the PP/fSiO<sub>2</sub> composite membrane was identified as a more potential membrane in gas-liquid membrane contactor applications than other commonly used polymeric membranes.

## CONCLUSIONS

In this research work, superhydrophobic composite PP membranes were prepared by a one-step sol-gel process. In order to investigate the effect of the sol-gel parameters on the wettability properties of the membranes, the molar ratio of PFOTES/TEOS was

varied from 0 to 1. The greatest static contact angle was obtained when the PFOTES/TEOS molar ratio was 0.5 which showed a water contact angle of 156°. Static wettability analyses confirmed that the PP/fSiO<sub>2</sub> composite membranes show the least wetting problem when they were immersed into the water and also aqueous alkanolamine solutions such as DEA and MEA. Interestingly, the superhydrophobic property of the coated membrane is uniformly distributed on the surface as well as in the cross-section of the membrane.

Moreover, the obtained results showed that the PP/fSiO<sub>2</sub> composite membrane was identified as a more potential membrane in gas-liquid membrane contactor applications than other commonly used polymeric membranes.

## CONFLICTS OF INTEREST

None declared

## REFERENCES

1. Sheen Y-C, Chang W-H, Chen W-C, Chang Y-H, Huang Y-C, Chang F-C (2009) Non-fluorinated superamphiphobic surfaces through sol-gel processing of methyltriethoxysilane and tetraethoxysilane. *Mater Chem Phys* 114:63-68
2. Yan YY, Gao N, Barthlott W (2011) Mimicking natural superhydrophobic surfaces and grasping the wetting process: A review on recent progress in preparing superhydrophobic surfaces. *Adv Colloid Interfac* 169: 80-105
3. Lv Y, Yu X, Jia J, Tu S-T, Yan J, Dahlquist E (2012) Fabrication and characterization of superhydrophobic polypropylene hollow fiber

- membranes for carbon dioxide absorption. *Applied Energy* 90: 167-174
4. Zhang Y, Sunarso J, Liu S, Wang R (2013) Current status and development of membranes for CO<sub>2</sub>/CH<sub>4</sub> separation: A review. *Int J Greenh Gas Con* 12:84-107
  5. Ramezani M, Vaezi MR, Kazemzadeh A (2014) Preparation of silane-functionalized silica films via two-step dip coating sol-gel and evaluation of their superhydrophobic properties. *Appl Surf Sci* 317:147-153
  6. Mansourizadeh A, Ismail A (2009) Hollow fiber gas-liquid membrane contactors for acid gas capture: a review. *J Hazard Mater* 171: 38-53
  7. Zhang Y, Wang R (2013) Gas-liquid membrane contactors for acid gas removal: Recent advances and future challenges. *Curr Opin Chem Eng* 2: 255-262
  8. Hamdi A, Chalon J, Laurent P, Dodin B, Dogheche E, Champagne P (2021) Facile synthesis of fluorine-free, hydrophobic, and highly transparent coatings for self-cleaning applications. *J Coating Technol* 18: 807-818
  9. Zhang Y, Wang R (2013) Fabrication of novel polyetherimide-fluorinated silica organic-inorganic composite hollow fiber membranes intended for membrane contactor application. *J Membrane Sci* 443: 170-180
  10. Ganbavle VV, Bangi UK, Latthe SS, Mahadik SA, Rao AV (2011) Self-cleaning silica coatings on glass by single step sol-gel route. *Surf Coat Tech* 205: 5338-5344
  11. Xie Y-T, Chen J-R, Chen Y-T, Jiang B-C, Sie Z-H, Hsu H-Y, Chen T-L, Chiang Y-Y, Hsueh H-Y (2021) Sol-gel-derived hierarchically wrinkled mesoporous ceramics for enhancement of cell alignment. *Chem Eng J* 405: 126572-126583
  12. Arya S, Mahajan P, Mahajan S, Khosla A, Datt R, Gupta V, Young S-J, Oruganti SK (2021) Influence of processing parameters to control morphology and optical properties of Sol-Gel synthesized ZnO nanoparticles. *ECS J Solid State Sci Technol* 10: 023002
  13. Wang Y, He G, Shao Y, Zhang D, Ruan X, Xiao W, Li X, Wu X, Jiang X (2019) Enhanced performance of superhydrophobic polypropylene membrane with modified antifouling surface for high salinity water treatment. *Sep Purif Technol* 214: 11-20
  14. Amirabedi P, Yegani R, Hesarak AH (2017) Hydrophobicity optimization of polypropylene hollow fiber membrane by sol-gel process for CO<sub>2</sub> absorption in gas-liquid membrane contactor using response surface methodology. *Iran Polym J* 26: 431-443
  15. Amirabedi P, Akbari A, Yegani R (2019) Fabrication of hydrophobic PP/CH<sub>3</sub>SiO<sub>2</sub> composite hollow fiber membrane for membrane contactor application. *Sep Purif Technol* 228: 115689-115699
  16. Kaneko K, Yadav N, Takeuchi K, Maira B, Terano M, Taniike T (2014) Versatile strategy for fabrication of polypropylene nanocomposites with inorganic network structures based on catalyzed in-situ sol-gel reaction during melt mixing. *Compos Sci Technol* 102:120-125
  17. Zu L, Li R, Jin L, Lian H, Liu Y, Cui X (2014) Preparation and characterization of polypropylene/silica composite particle with interpenetrating network via hot emulsion sol-gel approach. *Progress in Natural Science: Mater Int* 24: 42-49
  18. Mosadegh-Sedghi S, Rodrigue D, Brisson J, Iliuta MC (2014) Wetting phenomenon in membrane contactors-causes and prevention. *J Membrane Sci* 452:332-353
  19. Chen S-L, Dong P, Yang G-H, Yang J-J (1996) Kinetics of formation of monodisperse colloidal silica particles through the hydrolysis and condensation of tetraethylorthosilicate. *Ind Eng Chem Res* 35: 4487-4493
  20. Ramezani M, Vaezi MR, Kazemzadeh A (2015) The influence of the hydrophobic agent, catalyst, solvent and water content on the wetting properties of the silica films prepared by one-step sol-gel method. *Appl Surf Sci* 326: 99-106
  21. Sukitpaneenit P, Chung T-S (2009) Molecular elucidation of morphology and mechanical properties of PVDF hollow fiber membranes from aspects of phase inversion, crystallization and rheology. *J Membrane Sci* 340: 192-205
  22. Yegani R, Hirozawa H, Teramoto M, Himei H, Okada O, Takigawa T, Ohmura N, Matsumiya N, Matsuyama H (2007) Selective separation of CO<sub>2</sub> by using novel facilitated transport membrane at elevated temperatures and pressures.

- J Membrane Sci 291: 157-164
23. Rahim NA, Ghasem N, Al-Marzouqi M (2015) Absorption of CO<sub>2</sub> from natural gas using different amino acid salt solutions and regeneration using hollow fiber membrane contactors. *J Natural Gas Sci Eng* 26:108-117
  24. Yan S-p, Fang M-X, Zhang W-F, Wang S-Y, Xu Z-K, Luo Z-Y, Cen K-F (2007) Experimental study on the separation of CO<sub>2</sub> from flue gas using hollow fiber membrane contactors without wetting. *Fuel Process Technol* 88: 501-511
  25. Kumar M, Lawler J (2014) Preparation and characterization of negatively charged organic-inorganic hybrid ultrafiltration membranes for protein separation. *Sep Purif Technol* 130: 112-123
  26. Wang S, Guo X, Xie Y, Liu L, Yang H, Zhu R, Gong J, Peng L, Ding W (2012) Preparation of superhydrophobic silica film on Mg-Nd-Zn-Zr magnesium alloy with enhanced corrosion resistance by combining micro-arc oxidation and sol-gel method. *Surf Coat Tech* 213: 192-201
  27. Pavia DL, Lampman GM, Kriz GS, Vyvyan JA (2014) Introduction to spectroscopy, 5<sup>th</sup> ed., Cengage Learning
  28. Rahim NA, Ghasem N, Al-Marzouqi M (2015) Absorption of CO<sub>2</sub> from natural gas using different amino acid salt solutions and regeneration using hollow fiber membrane contactors. *J Natural Gas Sci Eng* 26: 108-117
  29. Wongchitphimon S, Wang R, Jiraratananon R (2011) Surface modification of polyvinylidene fluoride-co-hexafluoropropylene (PVDF-HFP) hollow fiber membrane for membrane gas absorption. *J Membrane Sci* 381: 183-191
  30. Boributh S, Rongwong W, Assabumrungrat S, Laosiripojana N, Jiraratananon R (2012) Mathematical modeling and cascade design of hollow fiber membrane contactor for CO<sub>2</sub> absorption by monoethanolamine. *J Membrane Sci* 401: 175-189
  31. Zhang H-Y, Wang R, Liang DT, Tay J (2008) Theoretical and experimental studies of membrane wetting in the membrane gas-liquid contacting process for CO<sub>2</sub> absorption. *J Membrane Sci* 308: 162-170
  32. Khaisri S, deMontigny D, Tontiwachwuthikul P, Jiraratananon R (2009) Comparing membrane resistance and absorption performance of three different membranes in a gas absorption membrane contactor. *Sep Purif Technol* 65: 290-297
  33. Wang R, Zhang HY, Feron PHM, Liang DT (2005) Influence of membrane wetting on CO<sub>2</sub> capture in microporous hollow fiber membrane contactors. *Sep Purif Technol* 46: 33-40
  34. Rahbari-Sisakht M, Ismail AF, Matsuura T (2012) Development of asymmetric polysulfone hollow fiber membrane contactor for CO<sub>2</sub> absorption. *Sep Purif Technol* 86:215-220
  35. Fosi-Kofal M, Mustafa A, Ismail AF, Rezaei-DashtArzhandi M, Matsuura T (2016) PVDF/CaCO<sub>3</sub> composite hollow fiber membrane for CO<sub>2</sub> absorption in gas-liquid membrane contactor. *J Natural Gas Sci Eng* 31: 428-436
  36. Mansourizadeh A, Ismail AF (2011) A developed asymmetric PVDF hollow fiber membrane structure for CO<sub>2</sub> absorption. *Int J Greenh Gas Con* 5: 374-380
  37. Mansourizadeh A, Ismail AF (2010) Effect of additives on the structure and performance of polysulfone hollow fiber membranes for CO<sub>2</sub> absorption. *J Membrane Sci* 348: 260-267